



Coupled dynamics of iron and iron-bound organic carbon in forest soils during anaerobic reduction



Qian Zhao^a, Dinesh Adhikari^a, Rixiang Huang^b, Aman Patel^c, Xilong Wang^d, Yuanzhi Tang^b, Daniel Obrist^e, Eric E. Roden^f, Yu Yang^{a,*}

^a Department of Civil and Environmental Engineering, University of Nevada-Reno, 89557, NV, USA

^b School of Earth and Atmospheric Sciences, Georgia Institute of Technology, Atlanta 30332, GA, USA

^c The Davidson Academy of Nevada, Reno 89557, NV, USA

^d Laboratory for Earth Surface Processes, College of Urban and Environmental Sciences, Peking University, Beijing 100871, PR China

^e Division of Atmospheric Sciences, Desert Research Institute, Reno 89512, NV, USA

^f Department of Geology and Geophysics, University of Wisconsin-Madison, 53706, WI, USA

ARTICLE INFO

Article history:

Received 31 August 2016

Received in revised form 6 December 2016

Accepted 9 December 2016

Available online 13 December 2016

Keywords:

Iron-bound organic carbon

Microbial reduction

Soil organic carbon stability

X-ray absorption spectroscopy

Electron accepting capacity

ABSTRACT

The behavior of iron (Fe)-bound organic carbon (OC) under anoxic conditions in natural soils and sediments represents a critical knowledge gap for understanding the biogeochemical cycles of OC and Fe. In this study, we investigated the dynamics of Fe and OC in four forest soils in the presence of the dissimilatory Fe-reducing bacterium, *Shewanella oneidensis* MR-1. Over an 8-day reduction period, 3.8–9.9% of total OC was released to solution in conjunction with the reduction of 12.5–37.7% of reactive Fe. The fraction of OC released was correlated with the fraction of Fe reduced, indicating that the reductive release was the controlling factor for the mobilization of OC upon the anaerobic microbial reaction. During the reduction, the fractions of poorly crystalline Fe oxides decreased, coupling with an increase in the relative abundance of crystalline Fe oxides. Lability of OC (as reflected by water-extractable OC content) increased after microbial reduction, indicating the decreased stability of OC because of changes in mineral-OC interactions and the conformation of mineral-OC complexes. The reduction of Fe was closely related to bulk soil electron accepting capacity (0.15–0.34 mmol e⁻/mol C). Our findings demonstrate that the redox reactions of Fe, modified by the redox reactivity of OC, play an important role in regulating the stability and transformation of OC.

© 2016 Elsevier B.V. All rights reserved.

1. Introduction

Iron (Fe) oxide minerals have been found to sorb and stabilize a substantial amount of organic carbon (OC) in natural soils and sediments (Wagai and Mayer, 2007; Lalonde et al., 2012; Zhao et al., 2016). Ferric oxide minerals were shown to have relatively high sorption affinity for OC as compared to other minerals (Tipping, 1981; Kaiser and Guggenberger, 2007). The sorption coefficients of dissolved organic carbon (DOC) on goethite and hematite were 2.6–4.0 and 0.85 mol C/kg, respectively, compared to the value of 0.1 mol C/kg for illite (Tipping, 1981; Kaiser et al., 1997). Poorly-crystalline Fe oxide, such as ferrihydrite (Fh), has even higher sorption coefficient of 7.1 mol C/kg (Kaiser et al., 1997). In addition to the sorption, poorly-crystalline Fe oxide can incorporate OC through co-precipitation (Kaiser et al., 1997). The Fh-OC complexes formed through co-precipitation would have much higher C/Fe compared to the complexes with OC sorbed on the Fh

surface (Chen et al., 2014; Gu et al., 1994, 1995). As a result of such sorptive and incorporative interactions, a substantial fraction of OC in soil is associated with Fe oxides. Wagai and Mayer (2007) showed that the Fe-bound OC contributed up to 34% of total OC (TOC) in soils collected mainly from North America. A recent study with 14 different forest soils from the United States determined that Fe oxide-bound OC contributed on average 37.8% of TOC (Zhao et al., 2016). Therefore, Fe-bound OC contributes significantly to soil C, and plays an important role in regulating the biogeochemical C cycles. To evaluate and predict the C cycles, it is critical to understand the fate of Fe-bound OC in soils.

The fate of Fe-bound OC can be greatly influenced by the reduction of ferric minerals, which will significantly change the speciation and structure of Fe minerals. Fh can be reductively converted to other crystalline Fe oxides, such as hematite and goethite (Hansel et al., 2003; Kukkadapu et al., 2003; Zachara et al., 2002). OC is actively involved in the reduction of Fe oxides as electron shuttle, donor or acceptor (Lovley et al., 1996, 1999; Scott et al., 1998; Kappler et al., 2004; Keller et al., 2009; Roden et al., 2010). Our recent study, together with published research, showed that the presence of OC inhibits the formation of secondary minerals during the reduction of Fh (Shimizu et al.,

* Corresponding author.

E-mail address: yuy@unr.edu (Y. Yang).

2013; Adhikari et al., 2016b). However, there was limited information about the fate of OC in natural soils upon the reduction of Fe minerals, although recent studies have pointed out the importance of reductive release in the fate of OC in natural soils (Thompson et al., 2006; Hall and Silver, 2013).

Herein, we investigated the release and transformation of Fe-bound OC in natural forest soils when they are exposed to anaerobic microbial reduction. We studied: 1) the kinetics of Fe reduction and OC release; 2) the transformation of Fe and OC; 3) the impact of OC physicochemical properties on the Fe reduction and OC release.

2. Methods & materials

2.1. Materials

Four soil samples (A, B, C, and D) with a range of fraction of Fe-bound OC to TOC (13.0–57.8%) were collected from four forests in the United States (Obrist et al., 2011, 2015; Obrist, 2012; Zhao et al., 2016) (Table 1). Detailed information about sampling, characterization, and analysis of Fe-bound OC in these four soils can be found in previous publications (Obrist et al., 2011, 2015; Obrist, 2012; Zhao et al., 2016). Briefly, surface soils (0–20 cm) were sampled from all sites with clean latex gloves and stainless steel equipment. All the soils were stored on ice before the transportation. The four soils were chosen to represent the range of Fe-bound OC amount in natural soils and different soil types. In our recent published study (Zhao et al., 2016), we have demonstrated that the fraction of Fe-bound OC in TOC in natural forest soils ranged from below detection limit (0.6%) to 57.8%, and OC:Fe molar ratio ranged 0.56–17.7. For soils A–D, the fraction of Fe-bound OC in TOC ranged 13%–57.8%, and OC:Fe ranged 0.9–17.7. The four soils belong to three different types of soils, including Mollisols (soil A), Inceptisols (soil B), and Spodosols (soils C and D). Especially for Spodosols, the soil is normally enriched in humus and Al/Fe oxides, and often experiences transitions between anaerobic and aerobic conditions (Buol et al., 2011); thus, coupled dynamics of Fe and C under anaerobic conditions are important for the fate of soil OC.

The concentration of reactive Fe and Fe-bound OC was measured by a dithionite-citric acid-bicarbonate (DCB) extraction, using sodium dithionite, citrate and bicarbonate (Mehra and Jackson, 1960; Wagai and Mayer, 2007; Lalonde et al., 2012; Zhao et al., 2016). DCB-extracted Fe was measured by an inductively coupled plasma-atomic emission spectroscopy (ICP-AES) (Varian-Vista AX CCD, Palo Alto, CA, USA). Fe-bound OC was determined as the OC released by the DCB reduction, calibrated by the OC released by a bicarbonate buffer control (Zhao et al., 2016). To minimize the influences of different indigenous microbial communities, soils were autoclaved for 15 min at 121 °C (Robertson et al., 1999; Stuckey et al., 2016). For this study focusing on the geochemical processes of Fe and OC, it is ideal to have natural soils with *Shewanella oneidensis* MR-1 (*S. oneidensis* MR-1) as the only microbial Fe reducer. We noticed residual microbial activity for Fe reduction, but did not pursue further sterilization, as our tests showed that additional autoclaving led to mineral phase transformation of Fe and minimal reduction even with MR-1 (Supporting Information (SI), Sterilization, Fig. S1).

2.2. Microbial reduction

A model dissimilatory metal reducing bacterium, *S. oneidensis* MR-1, was added to soils to drive reduction of Fe (Myers and Nealson, 1988). The bacterial strain was donated by Dr. Fendorf at Stanford University. *S. oneidensis* MR-1 was grown with 25 g/L Luria Broth (LB) medium (Difco Laboratories, Detroit, MI). Cultures were incubated at 30 °C for 16 h to reach the late stationary phase and harvested by centrifugation (10,000 rpm, 5 min). The cells were washed three times with 3 mM sodium bicarbonate buffer (pH 6.8). To make bicarbonate buffer, the deionized water was bubbled with pure N₂ for 1 h, and then NaHCO₃ was added with pH adjusted. The washed cells were re-suspended in 3 mM sodium bicarbonate buffer (pH 6.8) to achieve a cell density of 10^{8.5} cells/mL. Autoclaved soils were added at 1 g/20 mL. Treatments included *S. oneidensis* MR-1 amended soils with or without 6% H₂ as an electron donor (Roden and Wetzel, 2002; Meshulam-Simon et al., 2007; Luan et al., 2010), as well as unamended (no *S. oneidensis* MR-1 cells) controls with 6% H₂, or aerobic controls with added *S. oneidensis* MR-1 cells. The purposes of all controls are explained in SI, Table S1. At different intervals within 8 days, dissolved and sorbed Fe(II), as well as the DOC, were measured.

Dissolved Fe(II) was analyzed using the ferrozine assay (Stookey, 1970; Lovley and Phillips, 1986a). Briefly, the samples were centrifuged at 10,000 rpm for 10 min, and 0.4 mL of supernatant was mixed with 4 mL of 1 g/L ferrozine in 20 mM PIPES (piperazine-1,4-bis (2-ethanesulfonic acid)) buffer at pH 7 and shaken to homogenize. After 5 min, the solution was measured for the absorbance at 562 nm by an ultraviolet-visible spectrophotometer (UV-Vis) (Evolution 260 BIO, Thermo Scientific). Total Fe(II) concentration was measured by extracting all the Fe(II) with 0.5 M HCl (Lovley and Phillips, 1986b; Xu et al., 2016). DOC concentration of the supernatant was quantified by Shimadzu TOC-VCSH (Kyoto, KYT, Japan).

2.3. Water extractable OC

As an indicator for the lability of OC, water-extractable OC concentration was measured to represent the stability of OC before and after microbial reduction. Briefly, an aliquot of each autoclaved soil was mixed with DI water at a solid to solution ratio of 1:20. The soil slurry was shaken at 100 rpm for 12 h at room temperature and then centrifuged at 10,000 rpm for 10 min. DOC concentration of supernatant was quantified by Shimadzu TOC-VCSH (Kyoto, KYT, Japan).

2.4. Electron accepting capacity measurement

Electron accepting capacity of OC in forest soils was measured following previous studies (Roden et al., 2010; Lovley et al., 1996). Fe in forest soils was stripped by the DCB reduction (Mehra and Jackson, 1960; Wagai and Mayer, 2007; Lalonde et al., 2012; Zhao et al., 2016). Then the residual soils were washed by DI water and centrifuged at 10,000 rpm; this process was repeated 6 times to remove residual chemicals and re-oxidize OC that may be reduced by DCB treatment (Roden et al., 2010). Fe-stripped forest soils were then incubated with 10^{8.5} cells/mL *S. oneidensis* MR-1 in 20 mM PIPES buffer. Lactate

Table 1
Characteristics of four forest soils used in this study.

Soil	Location	Soil order	TOC conc. (mg/g)	Reactive Fe conc. (mg/g)	Fraction of Fe-bound OC in TOC (%)	OC:Fe molar ratio
A	Marysville, CA	Mollisols	30.1	19.3	13.0	0.9
B	Ravensdale, WA	Inceptisols	43.0	6.2	18.1	5.8
C	Hart, MI	Spodosols	30.0	2.7	36.7	17.1
D	Howland, ME	Spodosols	33.4	5.2	57.8	17.7

(20 mM) was added as electron donors under N₂ atmosphere. At different time intervals, 0.25 mL of unfiltered soil slurry was reacted with 2 mL of 5 mM Fe(III) complexed with nitrilotriacetic acid (Fe(III)-NTA) for 1 min (Roden et al., 2010; Lovley et al., 1996). The reacted slurry was then filtered with 0.2- μ m filters, and 0.4 mL of filtrate was mixed with 4 mL of 1 g/L ferrozine solution to measure Fe(II) concentration by UV assay described above. To measure the amount of electrons accepted by DOC, 0.5 mL of soil slurry was filtered through 0.2- μ m filters, and 0.25 mL of filtrate was reacted with 2 mL of 5 mM Fe(III)-NTA for 1 min. The generated Fe(II) was analyzed by the ferrozine assay. Electron accepting capacities of both solid-phase and solution-phase OC in forest soils were equal to Fe(II) concentrations measured here.

2.5. Characterization

2.5.1. X-ray photoelectron spectroscopy (XPS)

Transformation of OC during the microbial reduction was analyzed by XPS. The sample was measured by AXIS-Ultra instrument (Kratos Analytical Ltd., U.K.). XPS spectra of C 1s and Fe 2p were measured at a normal angle with respect to the plane of the surface. Binding energies were determined with an accuracy of ± 0.2 eV and calibrated by C 1s peak at 284.8 eV. Deconvolution of C 1s and Fe 2p spectra was done with CasaXPS software package. The binding energy of C1s XPS was assigned at 284.6 eV for C=C, 285 eV for C-C/C-H, 286.2 eV for C-O, 286.7 eV for C-O-C, 287.6 eV for C=O, and 289.1 eV for COO (Shin et al., 2009; Huang et al., 2011; Cheng et al., 2006; Proctor and Sherwood, 1982).

2.5.2. X-ray absorption spectroscopy (XAS)

Iron mineralogy in soil samples was examined by Fe K-edge XAS at beamline 4-1 of Stanford Synchrotron Radiation Lightsource (SSRL). A portion of the reacted samples was dried inside a glove box (94% N₂/6% H₂) and finely ground. Fine powders of both unreacted and reacted samples were spread on a Kapton tape and mounted on a sample holder inside a sample chamber that is purged with helium gas and cooled with liquid nitrogen to maintain anaerobic condition and minimize beam induced redox reaction. Energy calibration used an Fe foil (7112 eV). Data collection was conducted in both transmission and fluorescence mode (using a Lytle detector). Multiple spectra were collected for each sample and averaged. Data analysis used the software Sixpack (Webb, 2005) and Ifeffit (Newville, 2001). Principle component analysis was conducted on the data to evaluate the number of end member components needed for reconstructing the data. Identification and quantification of the unknown Fe phases were determined by target transformation and linear combination fitting (LCF) of the k^3 -weighted extended X-ray absorption fine structure (EXAFS) spectra of the unknown sample spectra at k range of 3–11 \AA^{-1} using a library of Fe reference compounds, including siderite, 2-line ferrihydrite, goethite, hematite, green rust, augite (Fe(III)-bearing aluminosilicates) (Hansel et al., 2003), as well as an Fe(III)-organic complex (Chen et al., 2014). Fe linear combinations of the empirical model spectra were optimized where the only adjustable parameters were the fractions of each model compound contributing to the fit. The goodness of fit was established by minimization of the R-factor (Newville, 2001).

2.5.3. Electron paramagnetic resonance (EPR) spectroscopy

EPR spectroscopy was used to study the dynamics of semi-quinone functional groups, which were suggested to be responsible for the extracellular electron transport (Lovley et al., 1996; Scott et al., 1998; Roden et al., 2010; Aeschbacher et al., 2010). The EPR spectra were recorded using a Bruker EMXPlus EPR spectrometer (Billerica, MA) at room temperature. A fixed amount (0.0016 g) of original and reduced soil was analyzed with microwave frequency of 9.38 GHz, microwave power of 20 dB (or 2.0 mW), sweep width of 200 G, and sweep time of 30 ms. Blank EPR tube was tested for baseline correction as well. The EPR signal area (X_{area}) was integrated using the software of Xenon

1.1b.44 version (Billerica, MA) as an index for the amount of semi-quinone functional groups.

2.6. Statistical analysis

Pearson correlation analyses were performed using IBM SPSS Statistics. Non-linear fitting for the kinetic data was conducted with MATLAB R2016a.

3. Results & discussion

3.1. Reduction of Fe

With H₂ as electron donor and added *S. oneidensis* MR-1 (biotic reduction sample), a substantial fraction of soil reactive Fe (12.5–37.7%), equal to 0.78–1.02 mg Fe/g soil, was reduced within 8 days (Fig. 1, SI, Fig. S2). The fraction of Fe reduction was not related to the amount of total reactive Fe (Pearson Correlation Coefficient $p = 0.57$, $r = 0.53$). Only a minor amount of Fe(II) was released to solution (≤ 0.11 mg/g soil), which accounted for <4.0% of total Fe(II) for all the four soils (SI, Fig. S2), mainly because of high sorption affinities of soil minerals for Fe(II) (Kaiser and Guggenberger, 2007; Chorover and Amistadi, 2001). These soils are mainly composed of quartz, aluminosilicates, and hematite minerals (SI, Fig. S3). Clay minerals can adsorb Fe(II) up to 64 mmol/kg clay (Géhin et al., 2007). Quantitatively, the reduction rate of total Fe ranged 0.07–0.45 mg Fe/g soil/day, when dissolved Fe(II) and sorbed Fe(II) were produced with the rate of 0.001–0.013 mg/g soil/day and 0.07–0.45 mg/g soil/day, respectively (SI, Table S2).

The aerobic control showed insignificant changes in both sorbed and dissolved Fe(II) concentrations. After reaction of 8 days, the differences between the fractions of total reduced Fe for biotic reduction sample and the control without 6% H₂ as an electron donor were 0.8%, 10%, 2.1% and 14.7% for soil A, B, C, and D, respectively. Such results indicate that for soil A and C, *S. oneidensis* MR-1 or residual native soil microbes could use soil organic matter as electron donors to reduce Fe(III). Without added *S. oneidensis* MR-1, up to 33.5% of total Fe was reduced in the presence of H₂. Published research and our recent study demonstrated minor abiotic Fe reduction by H₂ at pH = 7 (Christensen et al., 2000; Adhikari et al., 2016b). This indicates the residual native soil microbes were capable of reducing Fe within our experimental duration. The differences in fractions of total reduced Fe between the biotic reduction sample (with H₂ and added *S. oneidensis* MR-1) and control with no added *S. oneidensis* MR-1 in the presence of H₂ were 0.3%, 12.4%, 4.2%, and 21.1% for soil A, B, C, and D, respectively. These results indicate that for soil A and C, residual native microbes dominated Fe reduction, while for soil B and D, reduction was mainly performed by *S. oneidensis* MR-1. Measurement of CO₂ production in of *S. oneidensis* MR-1 amended soils with H₂ (SI, Fig. S4) indicated that respiration of soil organic carbon could account for most or all Fe reduction in each of the soils. Unfortunately, it is not possible to partition H₂ versus OC-driven Fe reduction in H₂-amended soils. However, the significant CO₂ production (via oxidation of soil OC) does provide an explanation for Fe reduction activity by soils A and C in the absence of H₂: it is well known that dissimilatory Fe(III)-reducing organisms such as *Shewanella* are unable to utilize complex OC under Fe(III)-reducing conditions (Lovley, 2000); thus Fe reduction in the absence of H₂ must have been linked to metabolism of native soil OC. Although this study focused on the geochemical processes for Fe and OC during anaerobic microbial reduction, the role and response of residual microbial communities warrant further investigations.

3.2. Release of OC

A substantial amount of OC was released to solution during Fe reduction. Originally, DOC ranged 0.67–1.38 mg C/g for soils A–D, as a result of

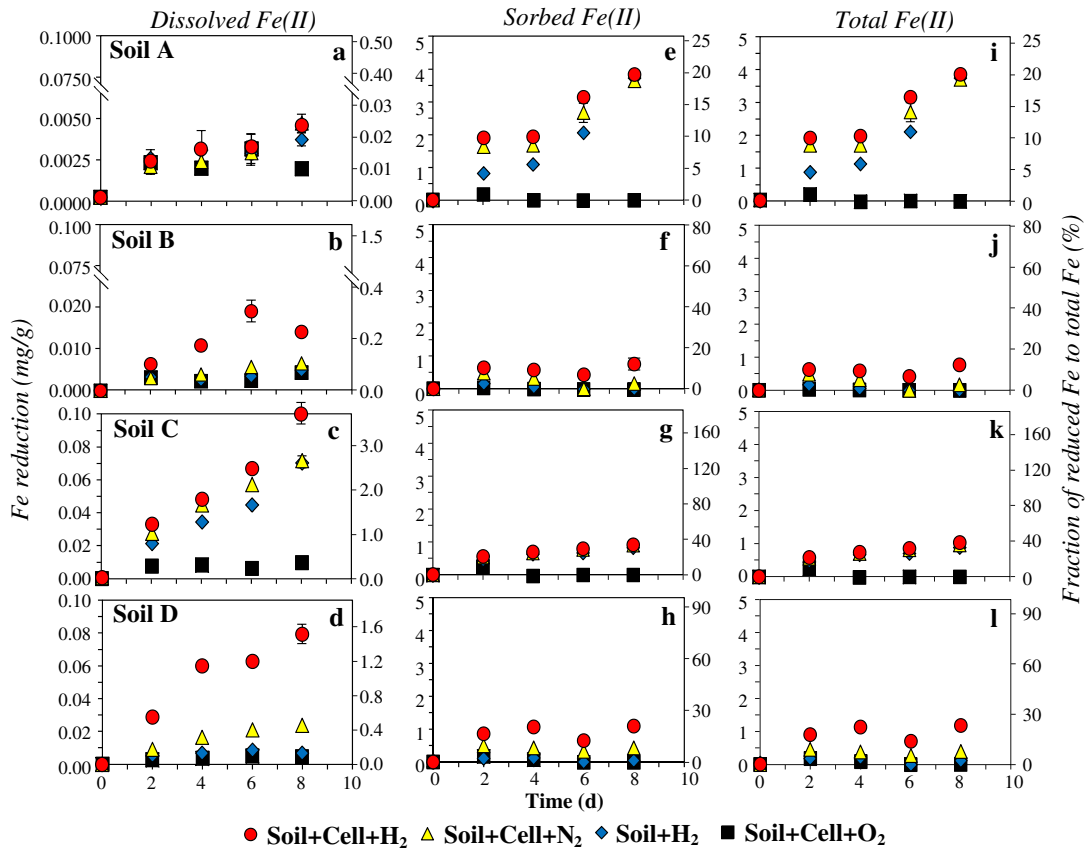


Fig. 1. Time-dependent dissolved (a–d), sorbed (e–h) and total (i–l) iron (Fe) (II) production for four forest soils (a, e, and i are soil A (Mollisols) located at Marysville, CA; b, f, and j are soil B (Inceptisols) located at Ravensdale, WA; c, g, and k are soil C (Spodosols) located at Hart, MI; d, h, and l are soil D (Spodosols) located at Howland, ME). The data represents measured Fe(II) concentrations minus Fe(II) at 0 day. (Error bars represent standard deviation calculated from triplicate experiments. Most are too small to visualize.)

repartitioning and desorption of OC into the solution phase. Between 1.62 and 2.98 mg OC/g soil was released as DOC during the 8-day incubation, corresponding to as much as 9.9% of TOC (Fig. 2, SI, Fig. S5). As a comparison, DOC in the aerobic control increased slightly with release

of up to 1.09 mg OC/g soil, which represented the contribution of microbial dissolution of OC and release of OC from microbial biomass and extracellular polymeric substances (EPS). The reductive release of OC was linear ($R^2 = 0.80–0.86$) over time, with the release rate of OC ranging

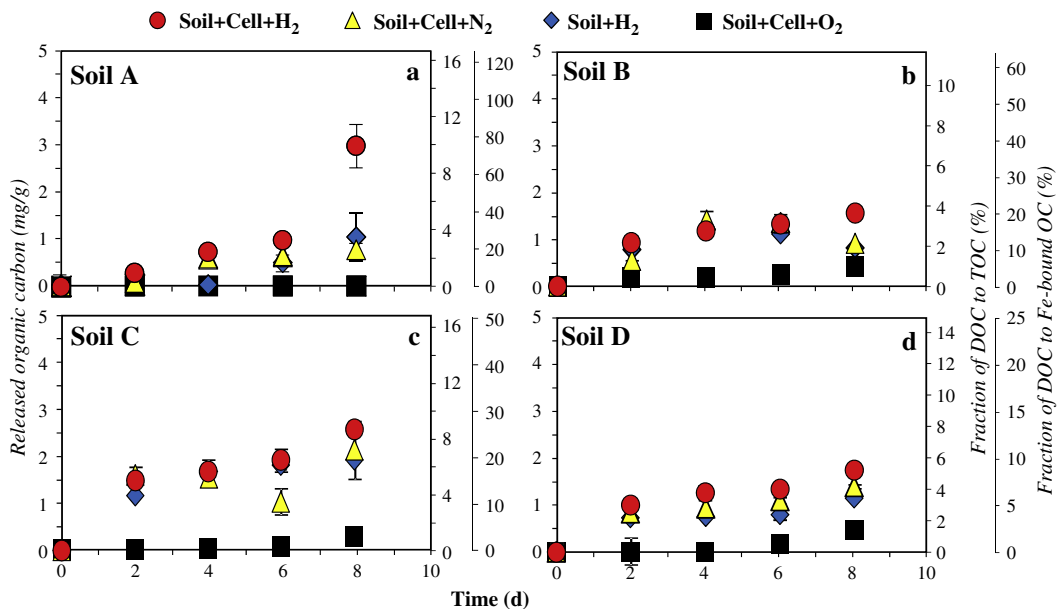


Fig. 2. Time-dependent dissolved organic carbon (DOC) release for four forest soils. The data represent measured DOC concentrations minus DOC at 0 day. The fractions of released DOC to total organic carbon (TOC) and Fe-bound organic carbon (OC) are showed on the right-hand y-axis.

0.18–0.33 mg/g/day (SI, Table S2). Although Fe reduction was similar with or without *S. oneidensis* MR-1 for soils B and D, the release of DOC was much higher for soils with added cells.

The fraction of TOC released to solution during Fe reduction was higher than the ratio of dissolved Fe(II) to total Fe(II) production, but smaller than the fraction of total Fe reduced: released DOC contributed to 3.8–9.9% of TOC, whereas 12.5–37.7% of Fe was reduced, with 0.02–4.0% of Fe(II) released to the solution phase. If we assume that all the DOC resulted from the release of Fe-bound OC, the released DOC accounted for 9.2–75.2% of Fe-bound OC. For soil A, the fraction of Fe-bound OC released was much higher than the reduction of Fe, while the reverse was true for soil D. The values for the Fe reduction and release of Fe-bound OC were similar for soils B and C. As a result of preferential release of OC, the molar ratio of DOC/total Fe(II) ranged between 3.6 and 11.8, higher than the C/Fe in the bulk soils (SI, Fig. S6). We defined a preferential release index (F_c) of freely dissolved OC (Eq. 1)

$$F_c = \frac{\text{DOC}}{\frac{\text{Fe(II)}_t}{\left(\frac{\text{C}}{\text{Fe}}\right)_{\text{bulk}}}} \quad (1)$$

where F_c is the preferential release index of freely dissolved OC, DOC is the molar concentration of dissolved organic carbon, Fe(II)_t is the molar concentration of total Fe(II), and $\left(\frac{\text{C}}{\text{Fe}}\right)_{\text{bulk}}$ is the molar C/Fe ratio in bulk soil. The value of F_c was 3.79, 1.66, 0.69, and 0.41 for soils A–D, respectively. We recently investigated the release of Fe-bound OC from synthesized Fe oxide-OC complexes. For hematite-OC complexes, our previous studies showed that the released fraction of Fe-bound OC was much higher than the reduction of Fe (Adhikari and Yang, 2015; Adhikari et al., 2016a). As a comparison, the relative release of Fh-bound OC compared to the reduction of Fe in Fh was dependent on the C/Fe ratio in Fh-OC complexes (Adhikari et al., 2016b).

Taking all the samples into consideration, concentration of released DOC correlated with the total Fe reduction ($r = 0.381$, $p = 0.001$) and concentration of sorbed Fe ($r = 0.361$, $p = 0.001$) (SI, Fig. S7, Table S3). The correlation between DOC and dissolved Fe(II) was even stronger ($r = 0.727$, $p < 0.001$) (SI, Fig. S7, Table S3). The fraction of DOC release relative to TOC was also closely related to the fraction of dissolved, sorbed and total Fe(II) in total Fe ($r = 0.65$ – 0.71 , $p < 0.001$). These correlations suggest DOC release was directly linked to Fe reduction, regardless of whether reduction was driven *S. oneidensis* MR-1 or the natural soil microflora.

3.3. Transformation of Fe

XRD spectra (SI, Fig. S3) showed that the dominating crystal mineral phase in four original bulk soils is quartz (31–80% sand content in the four soils). There are also contributions from clay minerals, including albite calcian, rhenium tantalum carbide, boron nitride, calcium manganese arsenide and sylvite. Fe minerals were rarely detected as bulk soil particles because of low concentrations of Fe (<1%). We did detect hematite in the clay fractions of soils A, indicating the concentrated Fe minerals in clay particles compared to bulk soil.

Fe K-edge X-ray absorption spectroscopy (XAS) analysis was employed to analyze Fe mineral phases in these forest soils more quantitatively. Analysis of the X-ray absorption near edge structure (XANES) region showed that the dominant oxidation state of Fe in all the unreacted soil samples are Fe(III), which can be identified by comparing the edge position (Fig. S8A) and first derivative peak positions (Fig. S8B) with the Fe(III) reference compound 2-line ferrihydrite and Fe(II) reference compound siderite (FeCO_3). Upon microbial reduction, the dominant Fe phase is still Fe(III) in soil A, slightly reduced for soil C, and dominated by Fe(II) phases in soils B and D, consistent with the relatively low fraction of sorbed Fe(II) in soil A compared to soil B–D (SI, Fig. S2).

Linear combination fitting (LCF) was conducted on the k^2 -weighted EXAFS data in the range of 3–11 \AA^{-1} for all four soil samples before and

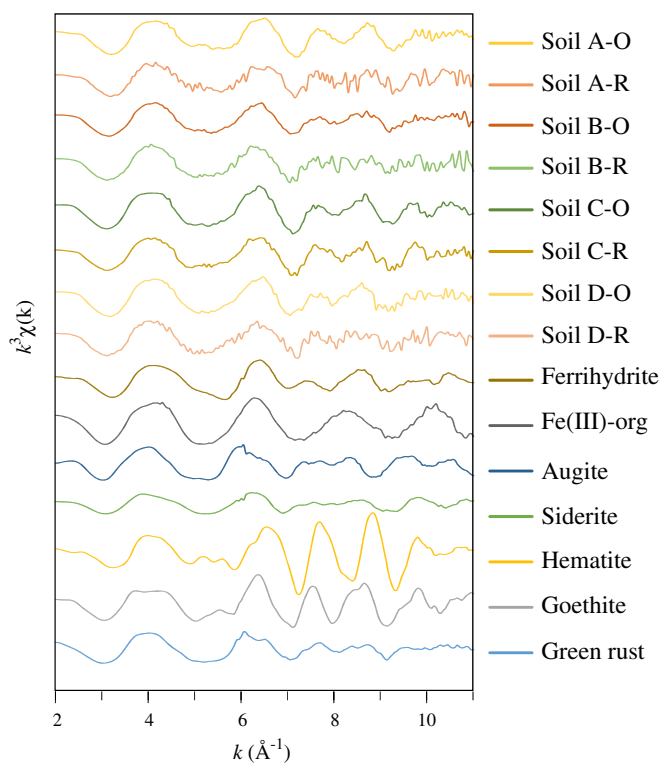


Fig. 3. Fe k^2 -weighted extended X-ray absorption fine structure (EXAFS) spectra of all the soils and Fe reference compounds used for linear combination fitting (LCF) over a k -range of 3–11 \AA^{-1} . O represents original soils and R refers to reduced soils incubated with *Shewanella oneidensis* MR-1 for 8 days.

after microbial reduction. Results are shown in Fig. 3; SI, Fig. S9, S10, Table S4. In all four unreacted soils, Fe(III)-bearing aluminosilicates, in the form of augite, accounted for 19–40% of total Fe, which is lower than the value of 46–50% for pasture soils (Chen et al., 2014). Augite is a single chain inosilicate mineral, and was used as a representative mineral phase for Fe(III) in less weathered aluminosilicate mineral phases. Fe oxides accounted for 66–85% of total Fe, with crystalline Fe oxides (e.g. hematite and goethite) contributing up to 49% of the total Fe and poorly crystalline Fe oxides (Fh) accounting for up to 56% of total Fe. For soil C and D, a significant portion of Fe was bound to soil organic matter (10–16%), which is supported by the higher fraction of Fe-bound OC in these soils (Table 1, Zhao et al., 2016). After microbial reduction, the fraction of Fh decreased by up to 23%, which indicates the microbial reduction preferentially used poorly-crystalline Fe oxides. Reduced Fe mineral phases such as siderite appeared after microbial reduction, consistent with XANES observations of the change of oxidation state from Fe(III) to Fe(II).

In addition to the bulk Fe speciation analysis, we also analyzed the composition of Fe minerals on particle surfaces using X-ray photoelectron spectroscopy. It is challenging to determine the species of Fe and transformation of Fe on the surface of soil particles, because of heterogeneity of soil particles and minor changes on the surface Fe species during the reduction process (SI, Fig. S11). Using the mineral phases of Fe determined from EXAFS analysis, we performed deconvolution to identify surface Fe species in soil A before and after reduction (SI, Fig. S12, Table S5), as soil A has the highest Fe content. The deconvolution results indicated that Fh contributed 38% to surface Fe, lower than the bulk fraction (56%) of Fh. After the reduction, the Fh decreased to 7% on the surface. The lower fraction of Fh on the surface is possibly due to its higher potential for reduction and mineral transformation (Weber et al., 2006), whereas Fh residing in the interior part of soil particles would be protected from transformation. Comparison between XPS analysis and EXAFS results uncovered the potential heterogeneous transformation of Fe on the surface and in the bulk of soil particles.

3.4. Transformation of OC

The water-extractable OC content of the four soils increased from 0.46 ± 0.14 mg/g to 0.98 ± 0.08 mg/g (mean \pm SD; $N = 4$) after reduction (SI, Fig. S13), corresponding to an increase in the fraction (relative to TOC) of water-extractable DOC from $1.40 \pm 0.53\%$ to $2.95 \pm 0.56\%$ ($N = 4$). Such changes could potentially have been partially influenced by release of DOC from microbial cells, indicated by increased water-extractable DOC from aerobic controls. However, the differences of water-extractable DOC between biotic reduction samples and aerobic controls demonstrated that microbial reduction appears to have interrupted interactions between OC and minerals, especially Fe oxides, making the originally strongly bound OC more mobile.

XPS analysis was conducted to gain insight into the chemical composition of surface-associated OC. The analysis showed that surface OC composition varied substantially among the four soils (Fig. 4). While the C=C functional group is one of the major components for all four soils, the peak diagnostic of C-O functional groups was more substantial for soils A, C and D. In soil D, there was also a significant peak at 289.1 eV, representing carboxylic functional groups. Quantitatively, C-O groups contributed 36.2, 22.9, 25.1, and 43.1% of total surface-associated OC for soils A, B, C, and D, respectively (SI, Table S6). After the reduction, the contribution of C-O increased to 39.5% and 52.3% for soil B and D, respectively, but decreased to 35.8% and 19.4% for soil A and C. The sorption of *S. oneidensis* MR-1 biomass to soil surfaces through interactions between soil minerals and cell-bound P-bearing lipid compounds may have contributed to the change in the surface C compositions (Persson et al., 1996; Salerno et al., 2004; Parikh and Chorover, 2006). However, previous studies have reported that the C1s XPS spectra of *S. oneidensis* MR-1 is dominated by C-C bonds, with

only minor contribution of C-O groups (Neal et al., 2002). Therefore, the change in XPS spectra were likely caused by changes in surface chemical composition of the soils. The increase in C-O functional groups after microbial reduction for soil B and D suggests that enrichment in hydrophilic moieties was associated with higher lability of surface-associated OC, as reflected by increased water-extractable OC content (SI, Fig. S13).

3.5. Electron accepting capacity of OC

The number of electrons accepted by the bulk soil slurry was much higher than that for filtered soil solution, indicating electrons were accepted by solid-phase OC (Fig. 5). The kinetics were fitted by a non-linear empirical model, and stable-level electron accepting capacities (EAC) based on the model fitting were used (SI, Table S7). Based on non-linear regression analysis of the time course data, the filtered soil solution accepted 0.12–0.15 mmol e⁻ equivalent/mol C at stable level, whereas the values were 0.27–0.49 mmol e⁻ equivalent/mol C for the bulk soil slurries (SI, Table S7). The difference indicates the EAC of solid-phase OC ranged from 0.15 to 0.34 mmol e⁻ equivalent/mol C. For soil A and C, the control of bulk soil slurries (not reacted with bacteria) also showed substantial increase in the electron accepted by OC, which implies that residual bacteria in soil A and C could also reduce soil OC. Roden et al. (2010) determined that the EAC of solid organic matter ranged between 0.13 and 0.41 mmol e⁻ equivalent/mol C for sediment samples collected from Talladega National Forest in Alabama, USA. Quinone groups have been identified as the most important moieties for the EAC of OC (Lovley et al., 1996; Scott et al., 1998; Roden et al., 2010; Aeschbacher et al., 2010). We detected EPR signal for soils A–D at a g value of 2.003, consistent with the position for the semi-quinone

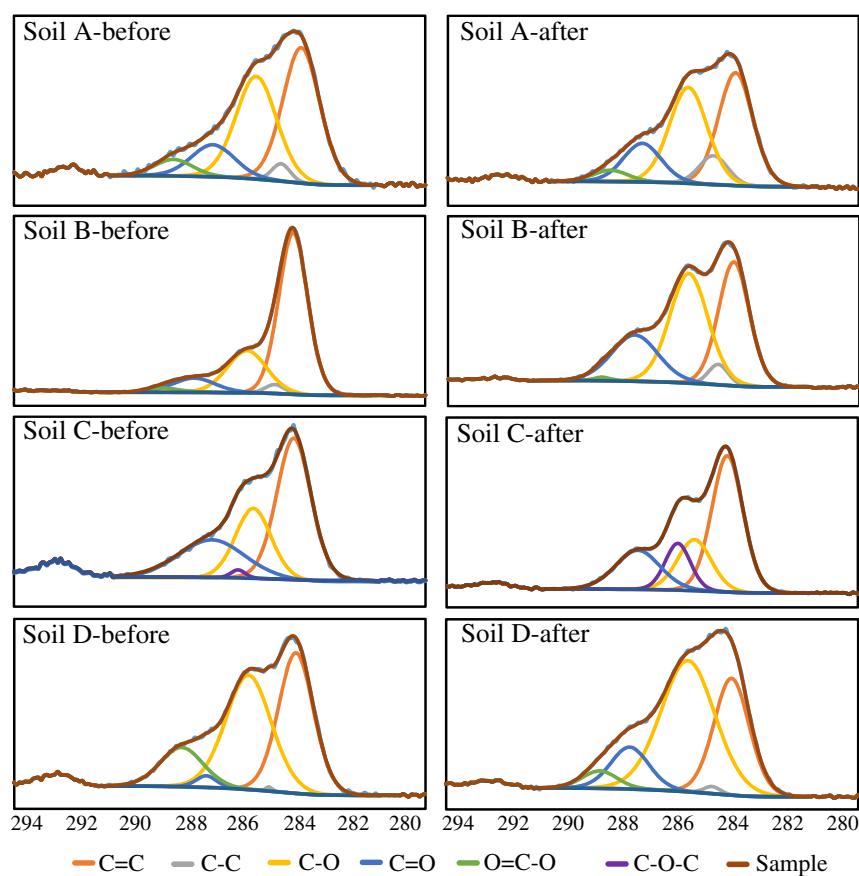


Fig. 4. Carbon (C) 1s X-ray photoelectron spectroscopy (XPS) spectra (solid lines) before and after anaerobic reduction. The deconvolutions of C1s XPS to the different components (dashed lines): the binding energy at 284.6 eV for C=C, 285 eV for C-C/C-H, 286.2 eV for C-O, 286.7 eV for C-O-C, 287.6 eV for C=O, and 289.1 eV for COO (Shin et al., 2009; Huang et al., 2011; Cheng et al., 2006; Proctor and Sherwood, 1982).

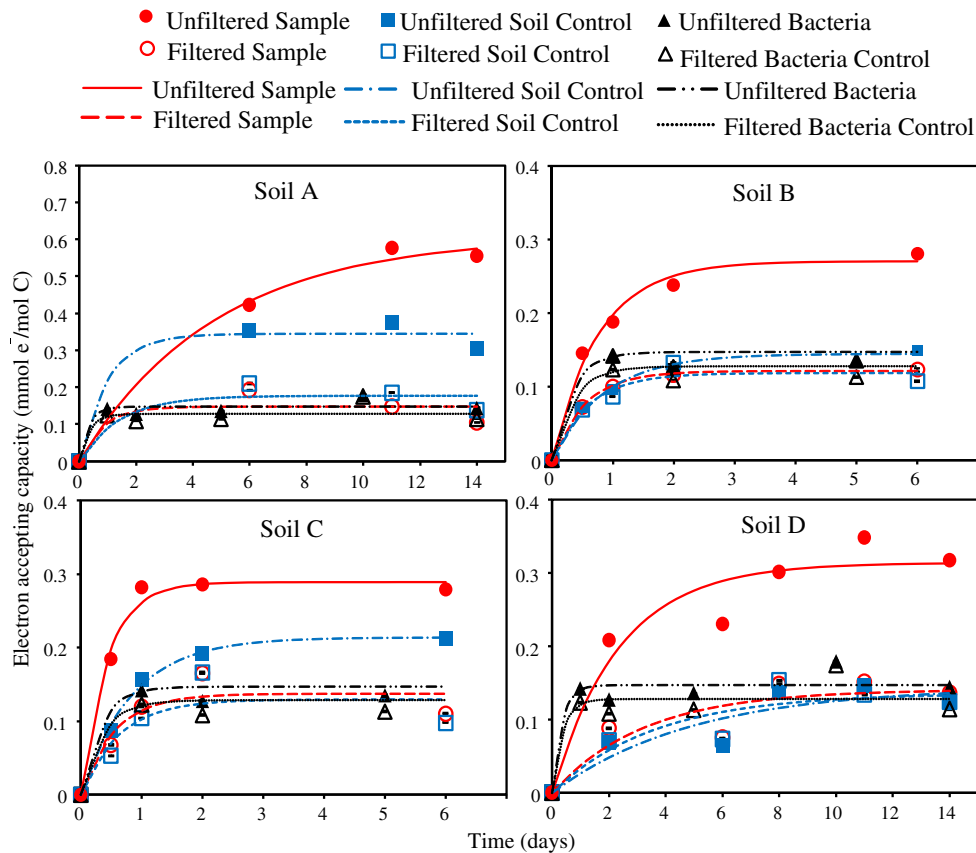


Fig. 5. Electron accepting capacity of organic carbon in Fe-stripped (see Materials & methods) forest soils during microbial reduction. Unfiltered and filtered samples refer to soil slurry reacted with Fe(III)-nitrilotriacetic acid (NTA) without and with filtration, respectively. Solid and dashed lines shown non-linear (first-order end product accumulation) least-squares regression fits to data for unfiltered and filtered samples, respectively.

functional groups (Knüpling et al., 1997). We found the highest EPR signal for semi-quinone groups in soil D, whereas the signal was minimal for other three soils (SI, Fig. S14). Although we cannot quantitatively determine the role of quinone groups in EAC of natural soils we used, there was an increase in semi-quinone functional groups during the microbial reduction process for soil D, indicating the involvement of quinone functional groups in the anaerobic redox reactions (SI, Fig. S15).

Finally, there was a significant positive correlation between both soil EAC and total Fe(II) produced during microbial reduction ($r = 0.726$, $p = 0.001$) (Fig. 6; SI, Fig. S16, Table S8). This indicates that electron

transfer from soil OC to Fe oxides (i.e. electron shuttling) enhanced Fe reduction.

4. Conclusion and environmental implications

We found that the release of OC under anaerobic conditions was closely related to the microbial reduction of Fe, indicating that the Fe reduction plays an important role in regulating the anaerobic mobilization of OC. Further investigations are warranted to determine the relative contribution of reductive release of soil OC, compared to other sources for DOC, such as microbial production (Bade et al., 2007; Högberg and Högberg, 2002; Hood et al., 2003). If we assume that the mobilized OC has higher availability for microbial degradation compared to soil particle-bound OC (Ohta et al., 1986; Nelson et al., 1994; Kalbitz et al., 2005), our results imply that microbial reduction of Fe can lead to mobilization and consequent faster degradation of OC in natural soils. The extent of Fe reduction was related to the EAC of OC in soil particles. This finding demonstrates that the biogeochemical cycles of Fe and OC can be coupled through complex, potentially synergistic interactions.

Our results also indicate that the fraction of poorly-crystalline Fe oxides was decreased during microbial reduction. Our previous studies together with other published research suggest the higher incorporation capacity of ferrihydrite compared to crystalline Fe oxides (Gu et al., 1994; Kaiser et al., 1997; Mikutta et al., 2005; Adhikari and Yang, 2015; Adhikari et al., 2016b; Chen et al., 2014). Reduction of ferrihydrite can drive substantial mobilization and transformation of OC, when the retained OC would become more mobile as the residual Fe oxides are more crystalline with less capacity for incorporating OC. Such changes in the Fe mineral phases during microbial reduction play an important role in regulating the fate of OC.

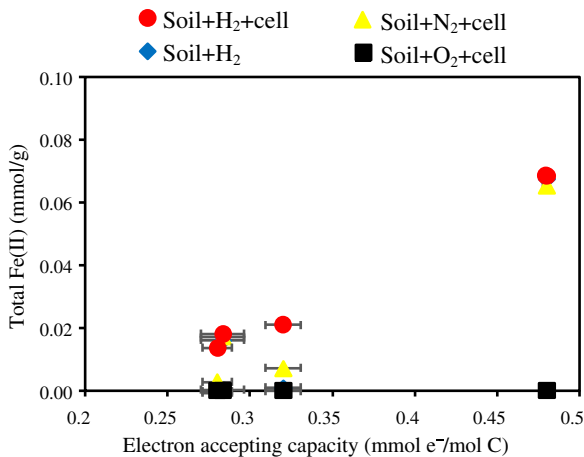


Fig. 6. Correlations between total Fe(II) produced during microbial reduction and the electron accepting capacity for the four forest soils. Error bars show standard deviations of both Fe reduction/OC release and electron accepting capacity from triplicate samples.

Acknowledgement

This research was financially supported by University of Nevada-Reno Startup fund, DOE grant DE-SC0014275 and USDA grant 2015-67018-23120. YT and RH acknowledge funding support from Georgia Institute of Technology and American Chemical Society Petroleum Research Fund (#54143-DN15). We appreciate the support from beamline scientist Ryan Davis at SSRL Beamline 4-1 on experimental setup. Portions of this research were conducted at the Stanford Synchrotron Radiation Lightsource (SSRL). SSRL is a Directorate of SLAC National Accelerator Laboratory and an Office of Science User Facility operated for the U.S. Department of Energy Office of Science by Stanford University. The support of the National Science Foundation (CHE-1429768) for the purchase of the powder X-ray diffractometer is gratefully acknowledged.

Appendix A. Supplementary data

Supplementary data to this article can be found online at <http://dx.doi.org/10.1016/j.chemgeo.2016.12.014>.

References

- Adhikari, D., Yang, Y., 2015. Selective stabilization of aliphatic organic carbon by iron oxide. *Sci. Rep.* 5.
- Adhikari, D., Poulson, S.R., Sumaila, S., Dynes, J.J., McBeth, J.M., Yang, Y., 2016a. Asynchronous reductive release of iron and organic carbon from hematite–humic acid complexes. *Chem. Geol.* 430, 13–20.
- Adhikari, D., Zhao, Q., Das, K., Mejia, J., Huang, R., Wang, X., Poulson, S.R., Tang, Y., Roden, E.E., Yang, Y., 2016b. Dynamics of ferrihydrite-bound organic carbon during microbial reduction (in review).
- Aeschbacher, M., Sander, M., Schwarzenbach, R.P., 2010. Novel electrochemical approach to assess the redox properties of humic substances. *Environ. Sci. Technol.* 44 (1), 87–93.
- Bade, D.L., Carpenter, S.R., Cole, J.J., Pace, M.L., Kritzbeg, E., Van de Bogert, M.C., Cory, R.M., McKnight, D.M., 2007. Sources and fates of dissolved organic carbon in lakes as determined by whole-lake carbon isotope additions. *Biogeochemistry* 84 (2), 115–129.
- Buol, S.W., Southard, R., Graham, R.C., McDaniel, P.A., 2011. Spodosols soils with subsoil accumulations of humus and sesquioxides. *Soil Genesis and Classification*, sixth ed. Wiley-Blackwell, Oxford.
- Chen, C., Dynes, J.J., Wang, J., Sparks, D.L., 2014. Properties of Fe-organic matter associations via coprecipitation versus adsorption. *Environ. Sci. Technol.* 48 (23), 13751–13759.
- Cheng, C.H., Lehmann, J., Thies, J.E., Burton, S.D., Engelhard, M.H., 2006. Oxidation of black carbon by biotic and abiotic processes. *Org. Geochem.* 37 (11), 1477–1488.
- Chorover, J., Amistadi, M.K., 2001. Reaction of forest floor organic matter at goethite, birnessite and smectite surfaces. *Geochim. Cosmochim. Acta* 65 (1), 95–109.
- Christensen, T.H., Bjerg, P.L., Banwart, S.A., Jakobsen, R., Heron, G., Albrechtsen, H.J., 2000. Characterization of redox conditions in groundwater contaminant plumes. *J. Contam. Hydrol.* 45 (3), 165–241.
- Géhin, A., Grenèche, J.M., Tournassat, C., Brendle, J., Rancourt, D.G., Charlet, L., 2007. Reversible surface-sorption-induced electron-transfer oxidation of Fe(II) at reactive sites on a synthetic clay mineral. *Geochim. Cosmochim. Acta* 71 (4), 863–876.
- Gu, B., Schmitt, J., Chen, Z., Liang, L., McCarthy, J.F., 1994. Adsorption and desorption of natural organic matter on iron oxide: mechanisms and models. *Environ. Sci. Technol.* 28 (1), 38–46.
- Gu, B., Schmitt, J., Chen, Z., Liang, L., McCarthy, J.F., 1995. Adsorption and desorption of different organic matter fractions on iron oxide. *Geochim. Cosmochim. Acta* 59 (2), 219–229.
- Hall, S.J., Silver, W.L., 2013. Iron oxidation stimulates organic matter decomposition in humid tropical forest soils. *Glob. Chang. Biol.* 19 (9), 2804–2813.
- Hansel, C.M., Benner, S.G., Neiss, J., Dohnalkova, A., Kukkadapu, R.K., Fendorf, S., 2003. Secondary mineralization pathways induced by dissimilatory iron reduction of ferrihydrite under advective flow. *Geochim. Cosmochim. Acta* 67 (16), 2977–2992.
- Högberg, M.N., Högberg, P., 2002. Extramatrical ectomycorrhizal mycelium contributes one third of microbial biomass and produces, together with associated roots, half the dissolved organic carbon in a forest soil. *New Phytol.* 154 (3), 791–795.
- Hood, E., McKnight, D.M., Williams, M.W., 2003. Sources and chemical character of dissolved organic carbon across an alpine/subalpine ecotone, Green Lakes Valley, Colorado Front Range, United States. *Water Resour. Res.* 39 (7), 1188.
- Huang, Y.L., Tien, H.W., Ma, C.C.M., Yang, S.Y., Wu, S.Y., Liu, H.Y., Mai, Y.W., 2011. Effect of extended polymer chains on properties of transparent graphene nanosheets conductive film. *J. Mater. Chem.* 21 (45), 18236–18241.
- Kaiser, K., Guggenberger, G., 2007. Sorptive stabilization of organic matter by microporous goethite: sorption into small pores vs. surface complexation. *Eur. J. Soil Sci.* 58 (1), 45–59.
- Kaiser, K., Guggenberger, G., Haumaier, L., Zech, W., 1997. Dissolved organic matter sorption on sub soils and minerals studied by ¹³C-NMR and DRIFT spectroscopy. *Eur. J. Soil Sci.* 48 (2), 301–310.
- Kalbitz, K., Schwesig, D., Rethemeyer, J., Matzner, E., 2005. Stabilization of dissolved organic matter by sorption to the mineral soil. *Soil Biol. Biochem.* 37 (7), 1319–1331.
- Kappler, A., Benz, M., Schink, B., Brune, A., 2004. Electron shuttling via humic acids in microbial iron(III) reduction in a freshwater sediment. *FEMS Microbiol. Ecol.* 47 (1), 85–92.
- Keller, J.K., Weisenhorn, P.B., Megonigal, J.P., 2009. Humic acids as electron acceptors in wetland decomposition. *Soil Biol. Biochem.* 41 (7), 1518–1522.
- Knüpling, M., Törring, J.T., Un, S., 1997. The relationship between the molecular structure of semiquinone radicals and their g-values. *Chem. Phys.* 219 (2), 291–304.
- Kukkadapu, R.K., Zachara, J.M., Fredrickson, J.K., Smith, S.C., Dohnalkova, A.C., Russell, C.K., 2003. Transformation of 2-line ferrihydrite to 6-line ferrihydrite under oxic and anoxic conditions. *Am. Mineral.* 88 (11–12), 1903–1914.
- Lalonde, K., Mucci, A., Ouellet, A., Gelin, Y., 2012. Preservation of organic matter in sediments promoted by iron. *Nature* 483 (7388), 198–200.
- Lovley, D.R., 2000. Fe(III) and Mn(IV) reduction. *Environmental Microbe-Metal Interactions*. ASM Press, Washington, DC, pp. 3–30.
- Lovley, D.R., Phillips, E.J., 1986a. Availability of ferric iron for microbial reduction in bottom sediments of the freshwater tidal Potomac River. *Appl. Environ. Microbiol.* 52 (4), 751–757.
- Lovley, D.R., Phillips, E.J., 1986b. Organic matter mineralization with reduction of ferric iron in anaerobic sediments. *Appl. Environ. Microbiol.* 51 (4), 683–689.
- Lovley, D.R., Coates, J.D., Blunt-Harris, E.L., Phillips, E.J.P., Woodward, J.C., 1996. Humic substances as electron acceptors for microbial respiration. *Nature* 382, 445–448.
- Lovley, D.R., Fraga, J.L., Coates, J.D., Blunt-Harris, E.L., 1999. Humics as an electron donor for anaerobic respiration. *Environ. Microbiol.* 1, 89–98.
- Luan, F., Burgos, W.D., Xie, L., Zhou, Q., 2010. Bioreduction of nitrobenzene, natural organic matter, and hematite by *Shewanella putrefaciens* CN32. *Environ. Sci. Technol.* 44 (1), 184–190.
- Mehra, O.P., Jackson, M.L., 1960. Iron oxide removal from soils and clays by a dithionite-citrate system buffered with sodium bicarbonate. *Clay Clay Miner.* 7, 317–327.
- Meshulam-Simon, G., Behrens, S., Choo, A.D., Spormann, A.M., 2007. Hydrogen metabolism in *Shewanella oneidensis* MR-1. *Appl. Environ. Microbiol.* 73 (4), 1153–1165.
- Mikutta, R., Kleber, M., Jahn, R., 2005. Poorly crystalline minerals protected organic carbon in clay subfractions from acid subsoil horizons. *Geoderma* 128 (1), 106–115.
- Myers, C.R., Nealson, K.H., 1988. Bacterial manganese reduction and growth with manganese oxide as the sole electron acceptor. *Science* 240 (4857), 1319–1321.
- Neal, A.L., Lowe, K., Daulton, T.L., Jones-Meehan, J., Little, B.J., 2002. Oxidation state of chromium associated with cell surfaces of *Shewanella oneidensis* during chromate reduction. *Appl. Surf. Sci.* 202 (3–4), 150–159.
- Nelson, P.N., Dector, M.C., Soulas, G., 1994. Availability of organic carbon in soluble and particle-size fractions from a soil profile. *Soil Biol. Biochem.* 26 (11), 1549–1555.
- Newville, M., 2001. IFEFFIT: interactive XAFS analysis and FEFF fitting. *J. Synchrotron Radiat.* 8 (2), 322–324.
- Obrist, D., 2012. Mercury distribution across 14 US forests, part II: patterns of methyl mercury concentrations and areal mass of total and methyl mercury. *Environ. Sci. Technol.* 46 (11), 5921–5930.
- Obrist, D., Johnson, D.W., Lindberg, S.E., Luo, Y., Hararuk, O., Bracho, R., Battles, J.J., Dail, D.B., Edmonds, R.L., Monson, R.K., Ollinger, S.V., Pallardy, S.G., Pregitzer, K.S., Todd, D.E., 2011. Mercury distribution across 14 US forests, part I: spatial patterns of concentrations in biomass, litter, and soils. *Environ. Sci. Technol.* 45 (9), 3974–3981.
- Obrist, D., Zielinska, B., Perlinger, J.A., 2015. Accumulation of polycyclic aromatic hydrocarbons (PAHs) and oxygenated PAHs (OPAHs) in organic and mineral soil horizons from four US remote forests. *Chemosphere* 134, 98–105.
- Ohta, S., Szuki, A., Kumada, K., 1986. Experimental studies on the behavior of fine organic particles and water-soluble organic matter in mineral soil horizons. *Soil Sci. Plant Nutr.* 32 (1), 15–26.
- Parikh, S.J., Chorover, J., 2006. ATR-FTIR spectroscopy reveals bond formation during bacterial adhesion to iron oxide. *Langmuir* 22 (20), 8492–8500.
- Persson, P., Nilsson, N., Sjöberg, S., 1996. Structure and bonding of orthophosphate ions at the iron oxide–aqueous interface. *J. Colloid Interface Sci.* 177 (1), 263–275.
- Proctor, A., Sherwood, P., 1982. XPS studies of carbon fiber surface. *Surf. Interface Anal.* 4, 213.
- Robertson, G.P., Coleman, D.C., Bledsoe, C.S., Sollins, P., 1999. *Standard Soil Methods for Long-term Ecological Research* (Vol. 2). Oxford University Press on Demand.
- Roden, E.E., Wetzel, R.G., 2002. Kinetics of microbial Fe(III) oxide reduction in freshwater wetland sediments. *Limnol. Oceanogr.* 47 (1), 198–211.
- Roden, E.E., Kappler, A., Bauer, I., Jiang, J., Paul, A., Stoesser, R., Konishi, H., Xu, H., 2010. Extracellular electron transfer through microbial reduction of solid-phase humic substances. *Nat. Geosci.* 3 (6), 417–421.
- Salerno, M.B., Logan, B.E., Velegol, D., 2004. Importance of molecular details in predicting bacterial adhesion to hydrophobic surfaces. *Langmuir* 20 (24), 10625–10629.
- Scott, D.T., McKnight, D.M., Blunt-Harris, E.L., Kolesar, S.E., Lovley, D.R., 1998. Quinone moieties act as electron acceptors in the reduction of humic substances by humics-reducing microorganisms. *Environ. Sci. Technol.* 32 (19), 2984–2989.
- Shimizu, M., Zhou, J., Schröder, C., Obst, M., Kappler, A., Borch, T., 2013. Dissimilatory reduction and transformation of ferrihydrite–humic acid coprecipitates. *Environ. Sci. Technol.* 47 (23), 13375–13384.
- Shin, H.J., Kim, K.K., Benayad, A., Yoon, S.M., Park, H.K., Jung, I.S., Jin, M.H., Jeong, H.K., Kim, J.M., Choi, J.Y., Lee, Y.H., 2009. Efficient reduction of graphite oxide by sodium borohydride and its effect on electrical conductance. *Adv. Funct. Mater.* 19 (12), 1987–1992.
- Stookey, L.L., 1970. Ferrozine—a new spectrophotometric reagent for iron. *Anal. Chem.* 42, 779–781.
- Stuckey, J.W., Schaefer, M.V., Kocar, B.D., Benner, S.G., Fendorf, S., 2016. Arsenic release metabolically limited to permanently water-saturated soil in Mekong Delta. *Nat. Geosci.* 9 (1), 70–76.

- Thompson, A., Chadwick, O.A., Rancourt, D.G., Chorover, J., 2006. Iron-oxide crystallinity increases during soil redox oscillations. *Geochim. Cosmochim. Acta* 70 (7), 1710–1727.
- Tipping, E., 1981. The adsorption of aquatic humic substances by iron oxides. *Geochim. Cosmochim. Acta* 45, 191–199.
- Wagai, R., Mayer, L.M., 2007. Sorptive stabilization of organic matter in soils by hydrous iron oxides. *Geochim. Cosmochim. Acta* 71 (1), 25–35.
- Webb, S.M., 2005. SIXpack: a graphical user interface for XAS analysis using IFEFFIT. *Phys. Scr.* 2005 (T115), 1011.
- Weber, K.A., Urrutia, M.M., Churchill, P.F., Kukkadapu, R.K., Roden, E.E., 2006. Anaerobic redox cycling of iron by freshwater sediment microorganisms. *Appl. Environ. Microbiol.* 8 (1), 100–113.
- Xu, S., Adhikari, D., Huang, R., Zhang, H., Tang, Y., Roden, E., Yang, Y., 2016. Biochar-facilitated microbial reduction of hematite. *Environ. Sci. Technol.* 50 (5), 2389–2395.
- Zachara, J.M., Kukkadapu, R.K., Fredrickson, J.K., Gorby, Y.A., Smith, S.C., 2002. Biomineralization of poorly crystalline Fe(III) oxides by dissimilatory metal reducing bacteria (DMRB). *Geomicrobiol. J.* 19 (2), 179–207.
- Zhao, Q., Poulson, S.R., Obrist, D., Sumaila, S., Dynes, J.J., McBeth, J.M., Yang, Y., 2016. Iron-bound organic carbon in forest soils: quantification and characterization. *Biogeosciences* 13, 4777–4788.